

Superconducting vortex profile from fixed point measurements the “Lazy Fisherman” tunneling microscopy method

A. Kohen, T. Cren, Th. Proslir, Y. Noat, W. Sacks, and D. Roditchev

Institut des Nanosciences de Paris, Universit s Paris 6 et 7, CNRS (UMR 75 88), 75015 Paris, France

F. Giubileo, F. Bobba, and A. M. Cucolo

Department of Physics, and INFN-SUPERMAT Laboratory, University of Salerno, via S. Allende, 84081 Baronissi (SA), Italy

N. Zhigadlo, S. M. Kazakov, and J. Karpinski

Solid State Physics Laboratory, ETH Zurich, CH-8093 Zurich, Switzerland

(Received 25 February 2005; accepted 28 April 2005; published online 18 May 2005)

We introduce a mode of operation for studying the vortex phase in superconductors using scanning tunneling microscopy (STM). While in the conventional STM method, the tip is scanned over a sample in which a fixed vortex pattern is prepared, in our “Lazy Fisherman” method the STM tip is kept fixed at a selected location while the vortices are being moved by varying the applied magnetic field. By continuously acquiring the local tunneling conductance spectra, $dI/dV(V)$, we detect the changes in the local density of states under the tip due to the vortex motion. With no need for scanning, the method permits one to extend the study of vortices to samples in which scanning is difficult or even impossible due to surface nonuniformity and allows one to study vortex dynamics. Using a statistical analysis of the spectra, we reconstruct the single vortex zero bias conductance profile. We apply the method to the c -axis face of a MgB_2 single crystal sample and obtain a vortex profile with a coherence length, ξ of 57 ± 2 nm.   2005 American Institute of Physics. [DOI: 10.1063/1.1939077]

In type II superconductors the magnetic field penetrates the superconducting (SC) material, above a certain field (H_{c1}), in the form of quantized flux bundles, known as vortices, each vortex carrying a flux quantum of $\phi_0 = hc/e$.¹ The vortices arrange themselves in a lattice and the SC order parameter (OP), $\Delta(\mathbf{r})$, becomes spatially inhomogeneous, having a zero value in the center of each vortex and rising to its maximum value in between the vortices. Several experimental methods were developed for studying the vortex lattice. Most methods exploit the spatial variations in the value of the local magnetic field and are therefore sensitive to changes occurring over a length scale set by the magnetic field penetration length, λ . These include: Bitter decoration,² magneto-optical microscopy,³ local hall microscopy,⁴ electron interference microscopy,⁵ and squid microscopy.⁶ A different approach was developed using a scanning tunneling microscope (STM).⁷ The STM is used to map the electronic density of states (DOS) as a function of position by scanning its tip over the sample. This enables one to view the vortex lattice based on the observed changes in the value of the zero bias conductance (ZBC) which manifest the changes in value of $\Delta(\mathbf{r})$. Therefore the method is sensitive to changes occurring on a length scale set by the SC coherence length, ξ . This, together with the STM’s ability to obtain atomic resolution in the topographic mode, results in images of extremely high spatial resolution. The method had been successfully used in a number of materials such as NbSe_2 ,⁷ BSCCO ,⁸ YBCO ,⁹ $\text{LuNi}_2\text{B}_2\text{C}$,¹⁰ and MgB_2 .¹¹ A main drawback of this method is that its use is limited to highly flat samples. Moreover the relatively large time needed for obtaining a single image (several minutes for a picture obtained at a single voltage up to hours for the full spectra) limits its use in the study of vortex dynamics.

In this letter we show how to extend the use of STM to samples in which scanning is difficult or even impossible by using a different mode of operation which we name the lazy fisherman method (LFM).¹² In LFM the difficulties involved in scanning are avoided by keeping the STM tip at a fixed position in which at zero field a clear SC spectra is observed. The different points within the vortex lattice are accessed by creating a vortex motion, induced by slowly changing the value of the applied field, as illustrated in Fig. 1(a). We show how by statistically analyzing the data measured at a single fixed point one can reconstruct the vortex profile and thus extract the SC coherence length. We apply the LFM to a c -axis oriented surface of a single crystal MgB_2 sample. We find that the measured data represent well a statistical ensemble sampled uniformly over the vortex unit cell. We reconstruct the vortex profile in MgB_2 and find the SC coherence length to be $\xi = 57 \pm 2$ nm in close agreement with the value of 51 nm obtained by Eskildsen *et al.*¹¹ using the conventional STM scanning method.

Single crystals of MgB_2 were grown by a high pressure method described in Ref. 13. The experiments were carried out on a low temperature Omicron STM. The tunneling junctions were achieved by approaching mechanically cut Pt/Ir tips to the c -axis oriented surface of the crystal. Due to the peculiar electronic structure of the material, c -axis tunneling allows to probe mainly the quasiparticle density of states in the π -band.^{11,14} The superconducting critical temperature was determined locally by measuring the evolution of the tunneling conductance spectra as a function of temperature, and was found to be 38.5 K. The field dependence of the tunneling conductance spectra $dI(V)/dV$ was obtained by fixing the STM tip in a selected location and continuously measuring local I – V tunneling curves while slowly sweeping

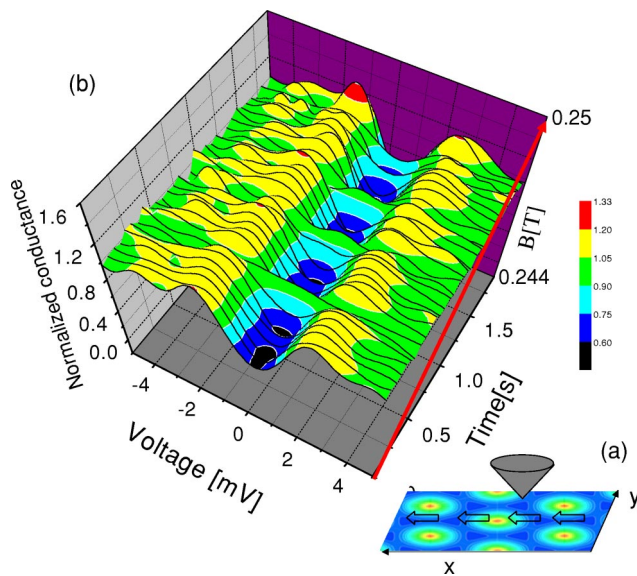


FIG. 1. (Color online) (a) Schematic drawing of the experimental method showing the STM tip (conic shape) fixed at a chosen position and the vortex motion (marked by arrows); (b) color coded 3D plot showing 30 normalized conductance spectra as a function of voltage and time exhibiting the variations in the local DOS under the tip induced by vortex motion. The magnetic field time dependence inducing the vortex motion is given by the thick line.

the magnetic field, the field being parallel to the c axis. At low temperature ($T=6.6$ K), the field was increased from zero up to the maximum value of 2.3 T at a rate of 0.15 T/min. The acquisition time for a single spectrum (-20 and 20 mV) was 60 ms. However the voltage range in which the DOS is effected by the vortex ($\pm\Delta \approx \pm 2$ mV), is scanned in only 6 ms. During such a short time the field may be considered constant for an individual spectra, as $\Delta B \approx 10^{-5}$ T, thus $\Delta B/B \ll 1$. As our measured spectra are symmetrical with respect to zero bias we conclude that, during the time required to obtain a single spectrum, the vortex motion is also negligible. However, subsequently measured spectra do differ as can be seen in Fig. 1(b) which shows an example of 30 consecutively acquired spectra obtained in the field range of 0.244–0.250 T. One clearly sees the non-monotonic changes in the local DOS under the tip, due to the vortex motion. The spectra range from a clearly gapped form showing shoulders at the gap edges (reflecting the DOS far from the vortex core) to a completely flat form (reflecting the DOS at the vortex core).

A commonly used parameter in conventional STM vortex mapping is the value of the normalized ZBC, $\sigma \equiv [dI/dV(V=0)]/[dI/dV(V \gg \Delta)]$. In the normal state this value is equal to 1 while in the SC state it is strongly reduced due to an opening of a gap in the DOS around the Fermi level. Thus, one obtains the vortex image by mapping the value of the ZBC as a function of position. The ZBC obtains its maximum value at the vortex core, gradually decreases as a function of the distance from the vortex core and reaches its minimum value at the point of equidistance from the vortices (see, for example, Ref. 11). Measuring the value of the ZBC as a function of the distance from the vortex core allows one to obtain the exact vortex profile and thus to estimate the SC coherence length, ξ .

As in our method one cannot directly determine the distance between the vortex core and the STM's tip we use a statistical method in order to study the distribution of the

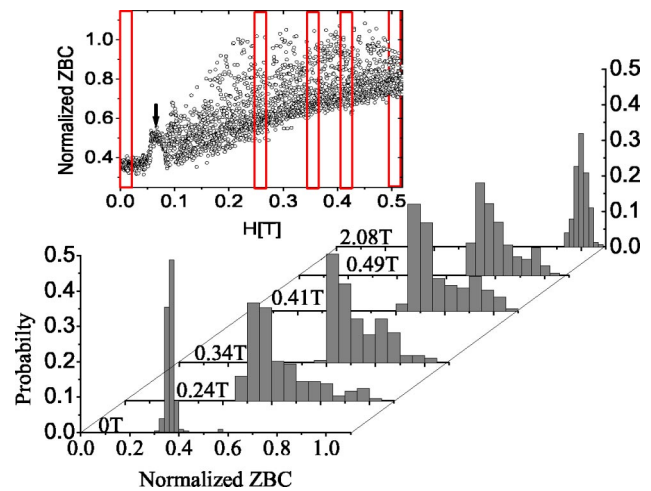


FIG. 2. Field evolution of the normalized ZBC histograms: 0, 0.24, 0.34, 0.41, 0.49, and 2.08 T. Histograms obtained at intermediate field values (0.24–0.49 T) show an asymmetric distribution peaked at or slightly above the minimum, reflecting the shape of the vortex profile. Inset shows the ZBC values obtained for $0 < H < 0.5$ T. Rectangles mark the ranges used for obtaining the histograms shown in the main figure.

ZBC values and to reconstruct the vortex profile. As a first step we have created histograms of the ZBC values acquired over 10 s intervals. The time interval was chosen to be on one hand short enough to assure that the intervortex distance does not significantly change ($\Delta d/d < 6\%$) and on the other hand to allow enough data points for statistical analysis.

The inset of Fig. 2 shows the ZBC values as a function of field for $0 < H < 0.5$ T. The field in which the vortex start to pass under the tip is clearly seen as a sharp jump in the values of the ZBC (see arrow in the inset). As this value is always larger than Hc_1 due to surface barrier effects we conclude that $Hc_{1||c} \approx 0.12 \pm 0.03$ T in agreement with the value of 0.1 T found by Lyard *et al.*¹⁵ by magnetization measurements. The resulting histograms at fields of 0, 0.24, 0.34, 0.41, 0.49, and 2.08 T are shown in Fig. 2. Each histogram represents roughly 150 ZBC values obtained in a field range of 0.03 T. The zero field histogram is narrow, symmetric and as expected shows no sign of spread in the ZBC values due to vortices. At higher fields ($H > 0.1$ T) the histograms become highly asymmetric. The probability is peaked near the minimum conductance value and decays considerably towards the maximum value. Looking at the set of histograms one can see an increase of the minimum value as the field increases, reflecting the increasing overlap between the vortices. In the case of MgB_2 the exact field dependence of this increase is rather complicated due to coupling between the two bands. We will discuss the properties related to the unique two band nature of MgB_2 in a separate publication.¹⁶ Finally at high fields ($H > 2$ T) the histogram becomes symmetric again with the modulation due to the vortices being so small that it is almost entirely washed out by the experimental noise. As no gap can be detected in any of our spectra for $H > 2.3$ T we deduce $H_{c2||c}(T=6.6 \text{ K}) \geq 2.3$ T, a value comparable to that measured by Lyard *et al.*¹⁵ of 2.6 T.

Using the ZBC histograms we are able to reconstruct, with no free parameters, the vortex profile, $ZBC(r) [= \sigma(r)]$, where r is the distance from the vortex core. Figure 3 shows the results calculated from the experimental histogram obtained in the field range of 0.24–0.27 T (see inset of Fig. 3). The abscissa which is the distance from the vortex core is

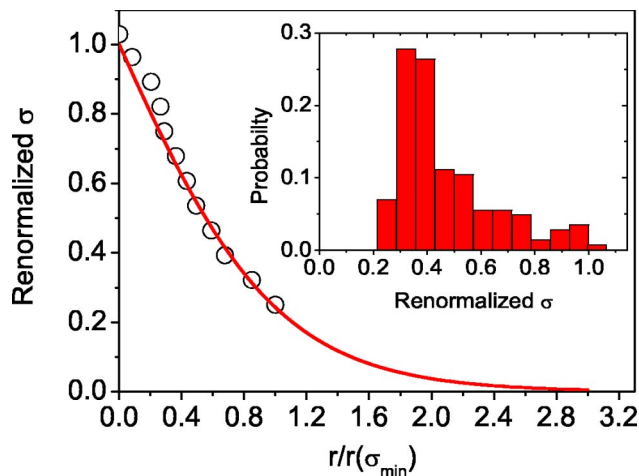


FIG. 3. Vortex profile, $\sigma(r)$ (circles) with a theoretical dependence given by $1 - \tanh(r/\xi)$ (line). Best fit is given by $\xi = 57 \pm 2$ nm. Inset shows the renormalized ZBC values histogram used to calculate the vortex profile.

calculated directly from the histogram using $r(\sigma_n)/r(\sigma_{\min}) = \sqrt{\sum_{i=n+1 \rightarrow N} P(\sigma_i, \sigma_i + \delta\sigma)}$, where $\delta\sigma$ is the bin size. This expression is exact for a vortex profile of cylindrical symmetry. In such a case the probability of obtaining a ZBC value between σ_1 and σ_2 which is general given by $P(\sigma_1, \sigma_2) \propto \int d\theta [r^2(\sigma_2, \theta) - r^2(\sigma_1, \theta)]$ reduces to $P(\sigma_1, \sigma_2) \propto [r^2(\sigma_2) - r^2(\sigma_1)]$. This approximation is valid as long as the intervortex distance is large in comparison to the coherence length ($\xi < d$) and that the material is in the dirty limit ($\xi > \ell$), which is the case in MgB_2 .¹¹ The ZBC is presented on a renormalized scale $[\sigma(H) - \sigma(H=0)]/[1 - \sigma(H=0)]$. This allows one to separate the contribution of DOS changes to the ZBC from that of finite temperature effects and inelastic tunneling process. The solid line in the figure is a best fit curve to the data obtained using $\sigma(r) = 1 - \tanh(r/\xi)$. The best fit is obtained for a value of $\xi/r(\sigma_{\min}) = 0.99 \pm 0.03$. As the minimum ZBC value is obtained (for a triangular lattice) at $r(\sigma_{\min}) = d/\sqrt{3} = 59$ nm (for $H = 0.24$ T), where d is the intervortex distance given by $d \approx 50$ nm/ \sqrt{H} , this results in $\xi = 57 \pm 2$ nm.

To conclude we have presented a method which allows to extend the use of STM for vortex study to cases where scanning is difficult or impossible and to cases showing fast vortex dynamics. Using the method one can measure several basic parameters describing the SC vortex state such as the field of first vortex penetration, the SC coherence length ξ and the upper critical field H_{c2} . At the same time our method

maintains the scanning capabilities of the STM. Thus, it allows repeating the measurement at different fixed points in the sample and relating the observed changes in vortex behavior to the position in the sample. This could be of interest in the vicinity of impurities, pinning centers, and grain boundaries. Additionally the LFM is suitable in all type of samples (rough and flat) for studying faster vortex dynamics (in comparison to conventional scanning) being limited only by the time needed to measure a single spectrum, ~ 1 ms. A variant of the method can be used for studying faster vortex dynamics by measuring the tunneling current (with open feedback loop) at a voltage of $eV \lesssim \Delta$. As vortex motion is the source of dissipation in the SC state, LFM being a local fast tool to study the SC parameters related to the vortex lattice and the vortex dynamics could of great use in the development of SC applications.

The authors thank Marco Aprili and Vincent Jeudi for useful discussions. This work has been supported by the Italian MIUR Project ‘‘Rientro dei Cervelli’’ and by the French University Paris 6 PPF Project.

- ¹A. A. Abrikosov, *Sov. Phys. JETP* **5**, 1174 (1957).
- ²F. Bitter, *Phys. Rev.* **38**, 1903 (1931).
- ³P. B. Alers, *Phys. Rev.* **105**, 104 (1957).
- ⁴P. Leiderer, P. Brüll, T. Klumpp, and B. Stritzker, *Physica B* **165–166**, 1387 (1990).
- ⁵T. Matsuda, S. Hasegawa, M. Igarashi, T. Kobayashi, M. Naito, H. Kajiya, J. Endo, N. Osakabe, A. Tonomura, and R. Aoki, *Phys. Rev. Lett.* **62**, 2519 (1989).
- ⁶J. R. Kirtely, M. B. Ketchen, K. G. Stawiasz, J. Z. Sun, W. J. Gallagher, S. H. Blanton, and S. J. Wind, *Appl. Phys. Lett.* **66**, 1138 (1995).
- ⁷H. F. Hess, R. B. Robinson, R. C. Dynes, J. M. Valles, Jr., and J. V. Waszczak, *Phys. Rev. Lett.* **62**, 214 (1989).
- ⁸S. H. Pan, E. W. Hudson, A. K. Gupta, K.-W. Ng, H. Eisaki, S. Uchida, and J. C. Davis, *Phys. Rev. Lett.* **85**, 1536 (2000).
- ⁹I. Maggio-Aprile, Ch. Renner, A. Erb, E. Walker, and O. Fischer, *Phys. Rev. Lett.* **75**, 2754 (1995).
- ¹⁰Y. De Wilde, M. Iavarone, U. Welp, V. Metlushko, A. E. Koshelev, I. Aranson, and G. W. Crabtree, *Phys. Rev. Lett.* **78**, 4273 (1997).
- ¹¹M. R. Eskildsen, M. Kugler, S. Tanaka, J. Jun, S. M. Kazakov, J. Karpinski, and O. Fischer, *Phys. Rev. Lett.* **89**, 187003 (2002).
- ¹²The name LFM is inspired by the resemblance of our method to that of a fisherman waiting stationary with his rod for passing by fish.
- ¹³J. Karpinski, M. Angst, J. Jun, S. M. Kazakov, R. Puzniak, A. Wisniewski, J. Roos, H. Keller, A. Perucchi, L. Degiorgi, M. Eskildsen, P. Bordet, L. Vinnikov, and A. Mironov, *Supercond. Sci. Technol.* **16**, 221 (2003).
- ¹⁴A. Brinkman, A. A. Golubov, H. Rogalla, O. V. Dolgov, J. Kortus, Y. Kong, O. Jepsen, and O. K. Andersen, *Phys. Rev. B* **65**, 180517 (2002).
- ¹⁵L. Lyard, P. Szab, T. Klein, J. Marcus, C. Marcenat, K. H. Kim, B. W. Kang, H. S. Lee, and S. I. Lee, *Phys. Rev. Lett.* **92**, 057001-1 (2004).
- ¹⁶A. Kohen, Th. Proslie, Y. Noat, F. Giubileo, F. Bobba, A. M. Cucolo, W. Sacks, and D. Roditchev (unpublished).